Earthquakes and Structures, *Vol. 10, No. 4 (2016) 789-810*
DOI: http://dx.doi.org/10.12989/eas.2016.10.4.789

Seismic fragility performance of skewed and curved bridges in low-to-moderate seismic region

Luke Chen[a] and Suren Chen[*]

Department of Civil and Environmental Engineering, Colorado State University, Fort Collins, CO 80523, USA

(Received February 27, 2015, Revised July 25, 2015, Accepted February 1, 2016)

Abstract. Reinforced concrete (RC) bridges with both skew and curvature are pretty common in areas with complex terrains. Existing studies have shown skewed and/or curved bridges exhibit more complicated seismic performance than straight bridges, and yet related seismic risk studies are still rare. These bridges deserve more studies in low-to-moderate seismic regions than those in seismic-prone areas. This is because for bridges with irregular and complex geometric designs, comprehensive seismic analysis is not always required and little knowledge about actual seismic risks for these bridges in low-to-moderate regions is available. To provide more insightful understanding of the seismic risks and the impact from the geometric configurations, analytical fragility studies are carried out on four typical bridge designs with different geometric configurations (i.e., straight, curved, skewed, skewed and curved) in the mountain west region of the United States. The results show the curved and skewed geometries can considerably affect the bridge seismic fragility in a complex manner, underscoring the importance of conducting detailed seismic risk assessment of skewed and curved bridges in low-to-moderate seismic regions.

Keywords: seismic; curved and skewed bridge; fragility; risk; FEM analysis

1. Introduction

Bridges are key components of modern transportation systems, which are typically classified as critical infrastructure. Based on rational vulnerability assessments, post-seismic functionality and serviceability of bridges can be evaluated, which directly affect the resilience of this type of critical infrastructure to seismic hazard. Seismic fragility analysis is a type of important seismic vulnerability assessment approach that can convert sophisticated seismic vulnerability of structures into a relation between conditional damage probability and ground motion intensity (e.g., Xiao and Ma 1997, Kowalsky and Priestley 2000, Ellingwood and Kinali 2009). Its concept is widely adopted not only in academic research fields, but also in engineering and risk management practices, such as HAZUS-MH by Federal Emergency Management Agency (FEMA) (Vickery *et al*. 2006). During the past twenty years, extensive work has been conducted on bridge fragility analyses, which were primarily focused on bridges with regular geometric configurations.

Horizontally curved and/or skewed bridges are often built to accommodate local terrain

*Corresponding author, Associate Professor, E-mail: suren.chen@colostate.edu
[a]Ph.D. Candidate, E-mail: neoluke@engr.colostate.edu

 ISSN: 2092-7614 (Print), 2092-7622 (Online)

constraints such as in the mountain west region of the United States. Fragility analyses of those bridges with special geometric features, such as curved and/or skewed bridges, are pretty limited. Sullivan and Nielson (2010) conducted sensitivity study of bridges with a variety of skewed angles and compared component responses in longitudinal and transverse directions. Zakeri *et al*. (2014) investigated the impacts of skew on the seismic performance of integral abutments and suggested that the component fragilities are independent of the geometric configuration if shear keys are added. It was found that bridges with skew and those with curvature share some common vulnerabilities, such as being susceptible to deck unseating, tangential joint damage, pounding effects as well as large in-plane deformation and rotations of the superstructure (Saiidi and Orie 1992, Maragakis 1984, Mwafy and Elnashi 2007). As compared to studies on bridges only with skew or with curvature, the seismic performance studies on bridges with combined curved and skewed geometric configurations are very rare. Wilson *et al*. (2014, 2015) studied the seismic dynamic performance of both skewed and curved bridges in the states of Colorado and Washington, respectively. The comparative results between the both curved and skewed bridges and their respective straight counterparts suggest that some unique trends deserve further studies in order to guide future designs of this type of irregular bridges against seismic.

Mountain west area in Colorado is a typical low-to-moderate seismic region. In the present study, fragility analysis is conducted on the representative bridges with both curved and skewed configurations selected from the mountain west region in Colorado. A suite of 3-D finite element models (FEM) for the bridge considering various uncertainties are built by modifying those originally developed by Wilson *et al*. (2014) with SAP2000. With both recorded and synthetic ground motions ranging from 0.1 g to 1.0 g Peak Ground Acceleration (PGA), nonlinear time history analyses of the bridge models are carried out considering uncertainties associated with ground motions and structural properties. Based on the time history analysis results, the Probability Seismic Demand Model (PSDM) and then fragility curves are further developed. Through the comparative studies of bridge models with four typical geometric configurations (i.e., straight, curved-only, skewed-only and both curved and skewed), the impacts of skew and curvature on the bridge fragility performance are assessed.

2. Bridge finite element modeling

2.1 Prototype bridge and its curved and skewed variations

A typical 3-span straight highway bridge on the interstate I-25 located in Denver Colorado is selected as the prototype bridge. The bridge has two identical side spans of 22.1 m each and a middle span of 29.5 m. Its superstructure is composed of 205 mm deep concrete slab deck supported by eight parallel pre-stressed concrete I-girders with 1.73 m depth and the integral connection is adopted to link the bridge deck and the abutment (Fig. 1(a)).

In order to study skewed and curved bridges based on realistic designs, some reasonable geometric variations from the straight prototype bridge were made (Wilson *et al*. 2014). For low-to-moderate seismic region, curved and/or skewed bridges often adopt the same design criteria as the straight counterparts when the curvature and/or skew are moderate. Therefore, the design details for these bridges with geometric variations are same as those for the prototype bridge. Such an arrangement has two advantages: (1) same design detail as the straight counterpart is pretty common for curved and skewed bridges in the region, yet without comprehensive evaluation in

(a) Prototype bridge (Graphic by Google Map)

(b) Straight bridge side view

(c) Straight bridge top view

(d) Skewed and curved bridge side view

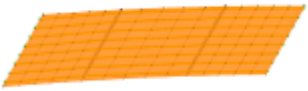

(e) Skewed and curved bridge top view

Fig. 1 Prototype 3D FEM bridge model and the variations (Wilson 2014)

Table 1 Geometric configurations of bridge model

Bridge type	Skew (degrees)	Curvature Radius (ft.)	Super Elevation (degrees)
Straight	0	0	0
Skewed only	30	0	0
Curved only	0	3000	6
Skewed and Curved	30	3000	6

terms of seismic performance and risk; (2) same designs of these bridge models allow for better investigations on the effects from geometric configurations by excluding other possible influences. As illustrated in Table 1, three representatives bridge models with different curved and skewed configurations (i.e., curved only, skewed only and both skewed and curved) are modified from the straight bridge model. The FEM analytical models of the straight prototype bridge and the curved and skewed bridge are shown in Figs. 1(b)-1(c) and Figs. 1(d)-(e), respectively. In the following sections, detailed fragility analyses are conducted for the four bridge models as listed in Table 1.

2.2 3-D finite element models

3-D FEM numerical models are developed with SAP2000 (CSI 2011) for the four bridge models listed in Table 1 (Wilson *et al*. 2014). Fig. 2 gives the modeling details of the bridge components including columns, integral abutments, bent caps and girders. The four semi-ellipse columns are labeled as column A-D, which are modeled as beam elements for both columns and pier caps with the bottom of the bridge pier fixed in the soil in all directions. In order to observe seismic inelastic response, plastic hinges are placed at both column ends with a relative distance suggested by the Washington State Department of Transportation Design Manual (WSDOT, 2002). Gaps between each span are simply supported by concrete bent cap rigidly connected with two RC columns on each side.

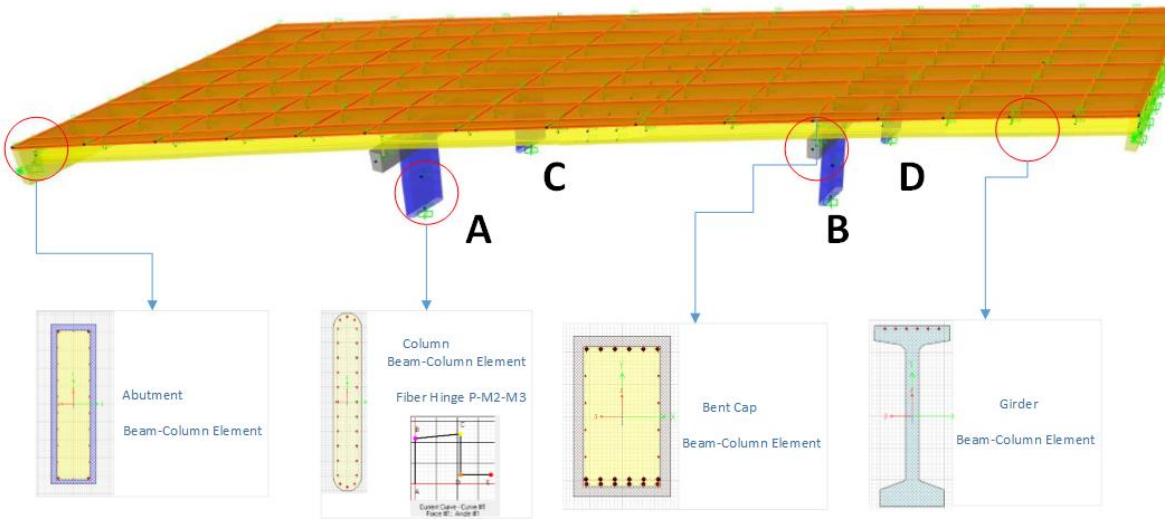

Fig. 2 Section modeling details

The integral abutments of the bridges are also modeled as beam elements with rigid connections to the end of the girders. Pile foundations of the abutments in all directions are fixed except for the longitudinal direction. Multi-linear compressive spring elements are applied in this direction based on the California Department of Transportation (Caltrans) design procedures for backing soil behind an integral abutment (Caltrans 2006). Plastic hinges with a lumped plasticity model are implemented at the top and bottom of the pier-columns to account for the inelastic column behavior of the substructure. In most of the bridge fragility analyses, superstructures were modeled with simplified elements or lumped as concentrate mass attached to the substructure. However, in order to capture the horizontal curvature characteristics in a better way, bridge decks are modeled as thin shell elements with 4 by 4 meshing. The eight girders are modeled as frame elements, which are connected with the bridge deck by use of fully constrained rigid links.

3. Uncertainties of bridge structures and sensitivity analysis

In order to conduct fragility analyses with limited samples, major uncertainties need to be appropriately considered. Most uncertainties associated with structures modeling can be classified into two categories: epistemic and aleatory uncertainties. The former one generally originates from model assumptions, simplified variables in formulas or lack of knowledge, which requires statistical uncertainties being incorporated into the numerical model. The later one is attributed to the inherent randomness in the seismic demand and capacity models, which means that the aleatory uncertainties should be considered when input ground motions or structural capacity models are selected.

Before incorporating structural uncertainties into the FEM models, an extensive sensitivity analysis is conducted to evaluate which variables are more critical in terms of considering uncertainties during the fragility curve development process. The sensitivity analysis is conducted under the excitation of the Whittier Narrows-01 earthquake (PGA=0.2 g). The results show that

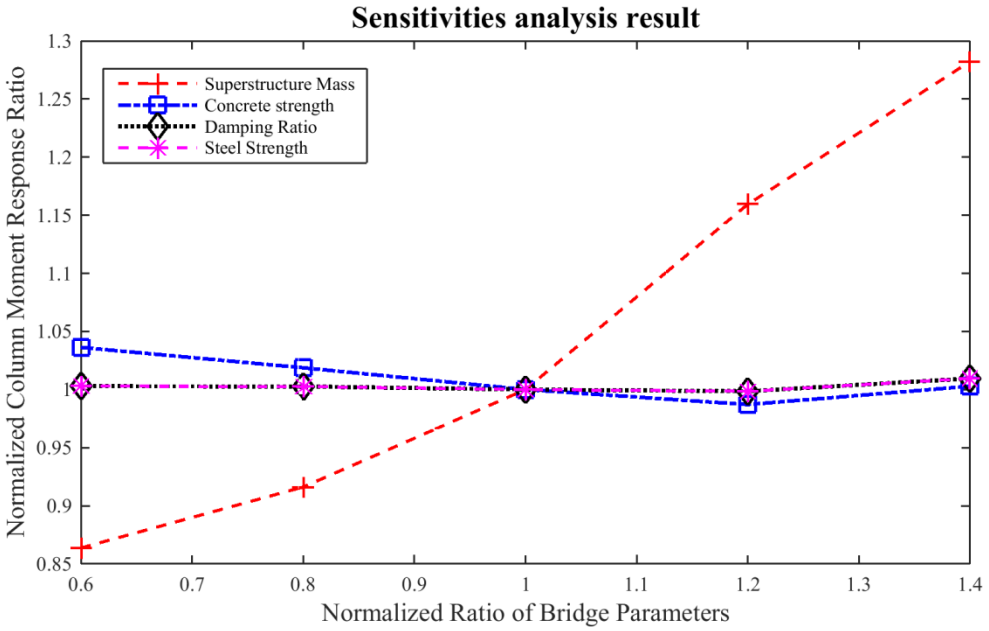

Fig. 3 Sensitivities analysis result

Table 2 Bridge uncertainties distribution

Bridge Parameter	Distribution Type	Mean	Deviation	Units	Reference
Compressive Concrete Strength	Normal	35.8	5.376	MPa	MacGregor *et al.* (1997)
Steel Yield Strength	Log-normal	463.3	37.07	MPa	Ellingwood and Hwang (1985)
Damping Ratio	normal	0.045	0.0125		Fang *et al.*(1999)
Superstructure Weight	Uniform	0.9–1.1	0		Nielson (2005)

concrete strength, steel yield strength, damping ratio and superstructure weight affect the bridge seismic performance pretty significantly and should be included into the models with considerations of uncertainties (Fig. 3).

In the absence of site-specific data, the uncertainty distributions of the variables in this study are decided primarily based on a comprehensive literature review of similar variables in existing studies. Based on the site-specific conditions, several assumptions and modifications are made in order to accommodate the specific bridge conditions and the uncertainty results are summarized in Table 2. The selected parameters based on the sensitivity analysis are then assigned to the models using Latin Hypercube Sampling (LHS) approach (Neves *et al*. 2006). The sampling method is used to ensure the variables allocated to model parameters based on particular probability distributions within a small number of samples, which will eventually lower the epistemic uncertainties. After applying the LHS, variables can be formed into a matrix, of which each row represents one FEM model with uncertainties (Table 3). In this study, eight models are generated for different geometric configurations, each of which is paired with twelve ground motions, generating 96 data points in total.

Table 3 Bridge uncertainties assignment based on LHS

	Density	**f'_c (kip)**	**F_y (kip)**	**Damping ratio**
s	0.151436	5.5166	66.3596	0.064486
2	0.14665	4.6244	68.0511	0.051163
3	0.16435	5.4006	72.1427	0.044602
4	0.139488	5.1094	59.4386	0.039779
5	0.145969	5.8012	75.9749	0.035814
6	0.161118	5.2671	64.6231	0.025715
7	0.136277	5.0403	62.5961	0.046521
8	0.156359	4.9216	69.8798	0.056484

Note: **f'_c**=Compressive Concrete Strength (Kip); **F_y**=Steel Yield Strength (Kip)

3.1 Compressive concrete strength

Generally, the compressive concrete strength of bridges follows normal distributions, but its mean value can vary considerably over different regions in the U.S. For example, eastern states such as New York State use 20.7 MPa in their standard design, which results in the mean value of 27.2 MPa and a standard deviation of 4.24 MPa (Pan *et al*. 2007). However in Central and Southeastern United States (CSUS), concrete strength typically has the mean value of 33.5 MPa and standard deviation of 4.3 MPa (Nielson 2005). In this study, by considering the site-specific conditions, the mean and standard deviation of the concrete strength are assumed to be similar to those obtained from the 5-ksi class experimental data (MacGregor *et al*. 1997), which are 35.8 MPa and 5.376 MPa, respectively.

3.2 Steel yield strength

For composite material like concrete, the specific failure mode (e.g., shear failure or flexure failure) for RC columns is usually dependent on individual components of the composite material. Thus, the uncertainty characteristics of reinforced steel and concrete are considered separately in this study. According to the findings in the statistical study by Ellingwood and Hwang (1985), the strength characteristics of the rebar are adopted to represent the steel strength uncertainty. The steel strength follows lognormal distribution, with mean and standard deviation for steel strength being 463.3 MPa and 37.07 MPa, respectively.

3.3 Damping ratio

The prototype bridge used in this study falls into the category of Multi-Span Continuous Concrete Girder (MSCCG) Bridges. In Nielson's study (Nielson 2005), the damping ratio distribution for MSCCG was estimated based on the study results from tall building (Fang *et al*. 1999) and typical damping ratio for bridges (Bavirisetty *et al*. 2000). Without further site-specific data, the damping ratio in this study follows the results by Nelson (2005) with a normal distribution and the mean and standard deviation values of 0.045 and 0.0125 respectively.

3.4 Superstructure weight

Although the bridge superstructure typically has less direct effect from seismic ground motions as compared to substructure and thus tends to remain elastic behavior, its weight could still have considerable effects on the seismic performance due to horizontal curvature and asymmetric layouts. Following the findings by Nielson (2005), the uncertainty of superstructure weight is attributable to the material density of the bridge deck, which is assumed to have a uniform distribution for a ratio between 0.9 and 1.1.

4. Ground motion simulation

Ground motions used in this study are a set of 96 earthquake records consisting of 48 real and 48 synthetic ground motions as described in the following sections. In order to study the impacts of skew and curvature on the bridge seismic performance, an input ground motion combination of 100% intensity in longitudinal direction and 40% in transverse direction was found to control the time history analysis (Wilson *et al*. 2014), which is also adopted in the following study.

4.1 Ground motion from database record

In order to properly reflect the seismic geographic features of Colorado, local seismic characteristics such as magnitude, Joyner-Boore distance and shear wave velocity have been considered during the selection of earthquake records from the Pacific Earthquake Engineering Research Center (PEER) ground motion database. Earthquake selection with a range from 4.5 to 8.5 Richter magnitude covers low-to-high seismic intensity. Ground motions with Joyner-Boore distance from 20 km to 100 km are selected according to the study of the fault lines distribution in Colorado by Matthews (2003). For the ground motion shear wave velocities (Vs30), their selection criteria are determined by site soil condition, which is the default D class soil with a range from 600 to 1200 ft./s according to the AASHTO LRFD specification (AASHTO 2013). Table 4 shows a typical suit of ground motion records used in this study.

4.2 Synthetic ground motion

A reliable PSDM requires representative ground motion inputs for time-history analysis to reduce its aleatory uncertainties. In most of the interplate regions such as California, ground

Table 4 Ground motion records from PEER

Event	Year	Station	Longitudinal PGA (g)	Transverse PGA(g)
Morgan Hill	1984	SF Intern. Airport	0.04783	0.04781
Chalfant Valley-01	1986	Bishop - LADWP South St	0.12943	0.09441
Santa Barbara	1987	UCSB Goleta	0.34022	0.34022
Northridge	1994	5360 Saturn St., Los Angeles	0.42029	0.42029
Imperial Valley-06	1979	Delta	0.23776	0.35112
San Fernando	1971	LA - Hollywood Story FF	0.20988	0.17418

Table 5 Synthetic ground motions generated for this study

Magnitude	Rjb (km)	Longitudinal PGA (g)	Transverse PGA(g)
6.0	60	0.57925	0.42831
6.5	60	0.64219	0.47302
7.0	60	0.51839	0.36556
6.0	40	0.58859	0.44692
6.5	40	0.70115	0.46789
7.0	40	0.81668	0.6134

motions can be selected from the database including PEER or U.S. Geological Survey (USGS) covering low to high seismic intensities. The mountain west region is lack of strong ground motion records and therefore synthetic ground motions are widely applied in fragility curve studies of the areas without sufficient seismic records (Choi 2002, Nielson and DesRoches 2007, Padgett and DesRoches 2007). Synthetic ground motions generated for this study follow Nielson's work (2005) with modification developed by Baker and Cornell (2005) in order to have a good coverage of different intensities. The generation procedure of synthetic ground motions is briefly introduced as follows: (1) Synthetic accelerograms are generated based on the determined parameters and corrected in frequency domain; (2) accelerograms are then adjusted to the site-specific target response spectrum according to the USGS map; and (3) every single synthetic ground motion is then used as a "seed" ground motion to generate orthogonal ground motions using correlation factors (Baker and Cornell 2005). Table 5 shows the selected synthetic ground motions generated in this study.

5. Fragility analysis

The first step to generate fragility curves is to establish probability seismic demand model (PSDM). According to the study by Baker and Cornell (2006), the median of structural demand S_d can be statistically described as exponential distribution

$$S_d = a * PGA^b \tag{1a}$$

or

$$\ln(S_d) = \ln(a) + b * \ln(PGA) \tag{1b}$$

where coefficients "a" and "b" can be determined by the regression analysis of the data points obtained from time history analysis.

Based on Eqs. (1a)-(1b), the cumulative conditional probability distribution of seismic demand exceeding certain level of structural capacity C under the corresponding seismic intensity can be written once the standard deviation $b_{D|IM}$ is estimated

$$P[D \geq C \mid IM] = 1 - \Phi\left(\frac{\ln(d) - \ln(aIM^b)}{\beta_{D|IM}}\right) \tag{2}$$

where $P[D \geq C \mid IM]$=the conditional probability that the seismic demand of structure (D) is greater than structural capacity (C) under specific seismic intensity (IM). $\Phi(.)$=the standard normal cumulative distribution function. S_d=median value of seismic demand of the pre-defined limit state.

With the assumption that the structural capacity and its seismic demand both have lognormal distributions, the concept of demand/capacity ratio is incorporated into Eq. (2) (Nielson 2005)

$$P[D \geq C \mid IM] = \Phi\left(\frac{\ln(S_d / S_c)}{\sqrt{\beta_{D|IM}^2 + \beta_c^2}}\right) \tag{3}$$

where S_c=median of the estimated capacity of the pre-defined limit state; β_c=standard deviation of the estimated capacity; $\beta_{D|IM}$=seismic demand standard deviation under specific seismic intensity IM.

The key steps of developing the fragility curves are summarized as follows and also in the flowchart as shown in Fig. 4:

(1) Build 3-D FEM models for each bridge as listed in Table 1, including the straight bridge and also the curved and skewed variations. Based on the sensitivity analysis, finalize uncertainties being considered in the study and apply those variables with uncertainties to the developed models.

(2) Select representative ground motions with intensities distributed from low to high based on

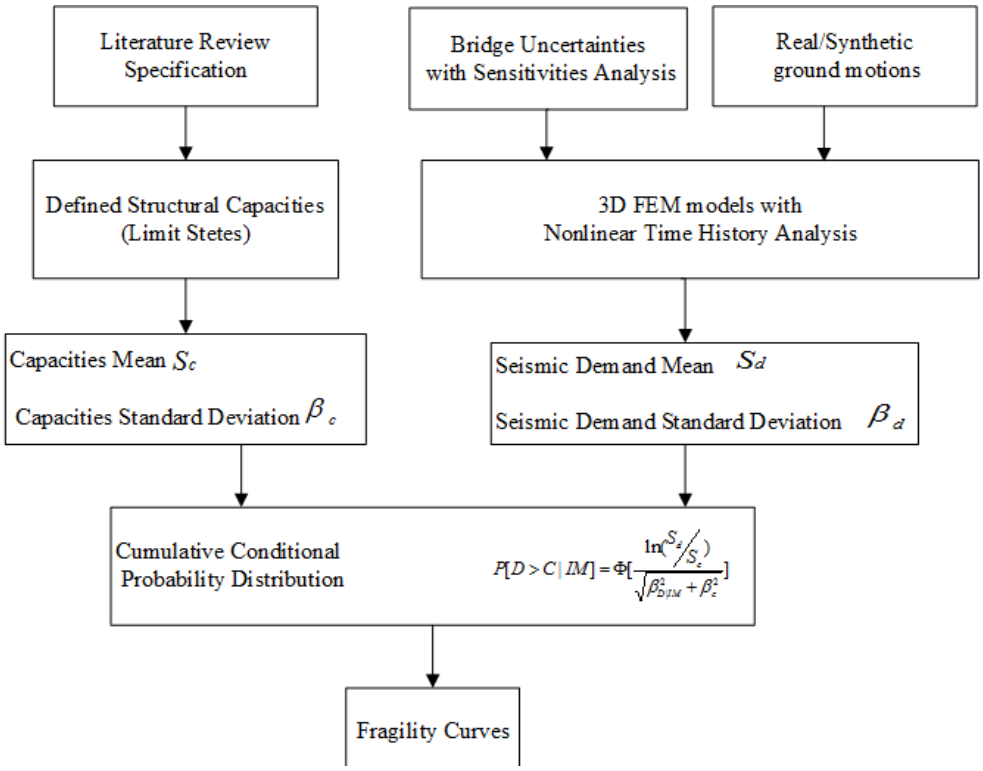

Fig. 4 Schematic diagram for component fragility curves construction

the site characteristics. If the ground motion from the database record is lacking, synthetic ground motions are generated for appropriate intensity coverage.

(3) Perform nonlinear time-history analyses on the FEM bridge models with uncertainties being considered, subjected to the representative ground motions. Obtain component seismic demands and apply regression analysis to obtain the coefficients "a" and "b" in Eq. (1b).

(4) Define appropriate structural limit states from literature, specifications and/or survey.

(5) Calculate analytical fragility curve following Eq. (3).

6. Limit states

Structural capacities discussed in the previous section are defined by limit states (or damage states), which determine the structural quantitative seismic demands causing damage to bridge components. In general, limit states can be determined through physics-based (e.g., experimental) approach, descriptive (e.g., expert survey) approach (Padgett and DesRoches 2007) or Bayesian approach (Nielson 2005). In this study, limit states are decided based on the literature review of the related studies and the selected ones are listed in Table 6 with details illustrated in the following.

Note: S_c =Median values of component limit states; β_c =dispersions of component limit states; Col-Long=column longitudinal curvature; Col-Trans=column transverse curvature; Shr-Long=Pier-Column Longitudinal shear strength; Shr-Trans=Pier-Column Transverse shear strength; Abut-a=abutment active deformation; Abut-p=abutment passive deformation; Wing=wing wall deformation.

6.1 Column moment curvature

Bridge columns are one of the critical components to seismic response that can result in different failure modes. In most of the fragility curve studies, flexural damage to bridge column is generally quantified based on the drift ratio (Shinozuka *et al*. 2002, Mackie and Stojadinović 2007, Zhang and Huo 2009) or ductility (Nielson and DesRoches 2007, Padgett and DesRoches 2008). For fragility analysis in this study, curvature ductility is determined as the limit state following the capacity estimation by Hwang's (2000) work and Federal Highway Administration's Seismic Retrofitting Manual for Highway Bridges (FHWA 1995). Hwang (2000) proposed limit states in

Table 6 Limit States used in the study with mean values and correlation factors

	Slight		**Moderate**		**Extensive**		**Complete**	
Component	S_c	β_c	S_c	β_c	S_c	β_c	S_c	β_c
Col-Long	0.0024515	0.59	0.0039908	0.51	0.0066893	0.64	0.009958	0.65
Col-Trans	0.0003359	0.59	0.0005467	0.51	0.0009164	0.64	0.0013642	0.65
Shr-Long (Kips)	N/A		N/A		N/A		731.59	N/A
Shr-Trans (Kips)	N/A		N/A		N/A		630.85	N/A
Abut-p (ft.)	0.1213911	0.25	0.2427822	0.25	0.8497375	0.46	2.4278215	0.46
Abut-a (ft.)	0.0593832	0.25	0.1190945	0.25	0.3569554	0.46	0.7139108	0.46
Wing (ft.)	0.1213911	0.25	0.2427822	0.25	0.8497375	0.46	2.4278215	0.46

terms of displacement ductility as 1.0, 1.2, 1.76 and 4.76 to respectively represent slight, moderate, extensive and complete damage states in FEMA (2003). The transformation equations for displacement ductility (μ_Δ) and curvature ductility (μ_ϕ) can be found in Ref (FHWA 1995)

$$\mu_\phi = 1 + \frac{\mu_\Delta - 1}{3\frac{l_p}{l}\left(1 - 0.5\frac{l_p}{l}\right)} \tag{4a}$$

where l is the column length and l_p is the plastic hinge follow by Eq. (4a) which is based on the diameter of the longitudinal reinforcement d_b

$$l_p = 0.08l + 9d_b \tag{4b}$$

The column ductility under light, moderate, extensive and complete damage states is defined with the mean values of 1.29, 2.1, 3.52 and 5.24, and with the corresponding parameter β_c of 0.59, 0.51, 0.64 and 0.65, respectively. The curvature ductility is later transfer into the curvature as shown in Table 6.

6.2 Pier-Column shear strength

Shear force on the bridge pier-column component is also one critical demand and could easily exceed its capacity during a seismic event. Because shear failure is a type of brittle failure and hard to be assessed with different serviceability conditions, only the complete damage state for shear strength in both directions is considered based on its damage model. The shear damage model considers the column concrete shear strength V_c, steel shear strength V_s and axial shear strength V_p (Priestley *et al*. 1996)

$$V_{total} = V_c + V_s + V_p \tag{5a}$$

where

$$V_c = k\sqrt{f_c}A_e \cong 0.232\sqrt{f_c}A_g \tag{5b}$$

$$V_s = \frac{A_{sw}f_y D'}{s}\cot\theta = \frac{A_{sw}f_y D'}{s}\cot 30^o \tag{5c}$$

$$V_p = \tan\alpha = \frac{D-c}{L}P \tag{5d}$$

f'_c=concrete compressive strength; A_g=section gross area; s=rebar spacing; L=rebar spacing; f_y=steel yield strength; D=section diameter; P=axial force; c=compression zone depth; D'=rebar diameter.

6.3 Abutment and wing-wall deformation

Abutment is another critical component for bridge seismic design, which has been often investigated in fragility studies (e.g., Kwon and Elnashai 2007, Billah *et al*. 2012). Deformation due to seismic ground motions not only cause failure to the back wall, but also enhance particular

behaviors such as pounding effect when skew is considered (Zakeri *et al*. 2014). According to the study by Choi (2002), passive deformation limit state of the integral abutment is defined as fraction of the maximum deformation capacity of the back fill soil (y_{max}) such as 0.005 y_{max}, 0.01 y_{max}, 0.35y_{max} and y_{max} for light, moderate, extensive and complete damage, respectively. In this study, y_{max} is assumed to be 2.42 ft. following the study by Sucuoğlu and Erberik (2004).

6.2 Regression analysis to develop PSDM

The time-history seismic analysis results of the selected structural components are represented as data points in the response-seismic intensity plots for nonlinear univariable regression analysis. According to the observation in the previous studies, it was found that most of the bridge models experience stacking effect on different columns, causing different seismic behavior on the interior and exterior columns (Wilson *et al*. 2014). Thus the regression analysis results for different columns are discussed individually.

With the assumption of lognormal distributions, the PSDM results of the longitudinal curvature for the skewed and curved bridge show considerable difference among different columns (Fig. 5). For comparison purposes, the longitudinal curvature PSDM results for the straight bridge are shown in Fig. 6. It is apparent that the PSDM results for the skewed and curved bridge are more scattered than those for the straight bridge. In the following fragility curve development, the differences among the regression lines of different columns will also be found to affect the results of probability distribution.

The PSDM results of the column-pier shear strength in the longitudinal and transverse directions for the skewed and curved bridge are shown in Figs. 7 and 8, respectively. The column shear PSDM results for the skewed and curved bridge also vary among different columns (Figs. 7-8) and the largest one can reach almost twice as that for the straight counterpart (not listed for the sake of brevity).

Fig. 9 shows the regression analysis results of the abutment deformation and wing wall response for the skewed and curved bridge. The passive and active longitudinal deformation only slightly vary from each other for the skewed and curved bridge. Table 7 summarizes the regression coefficients in Eq. (1) as well as their standard deviation "Beta" and coefficient of determination "R^2".

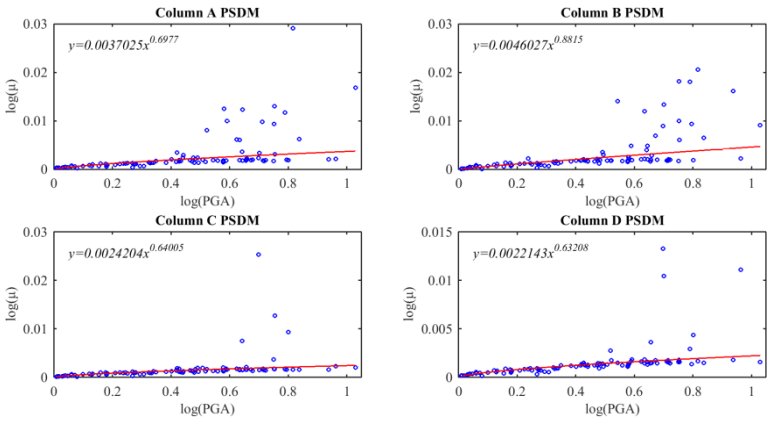

Fig. 5 Column longitudinal curvatures PSDM for the curved and skewed bridge

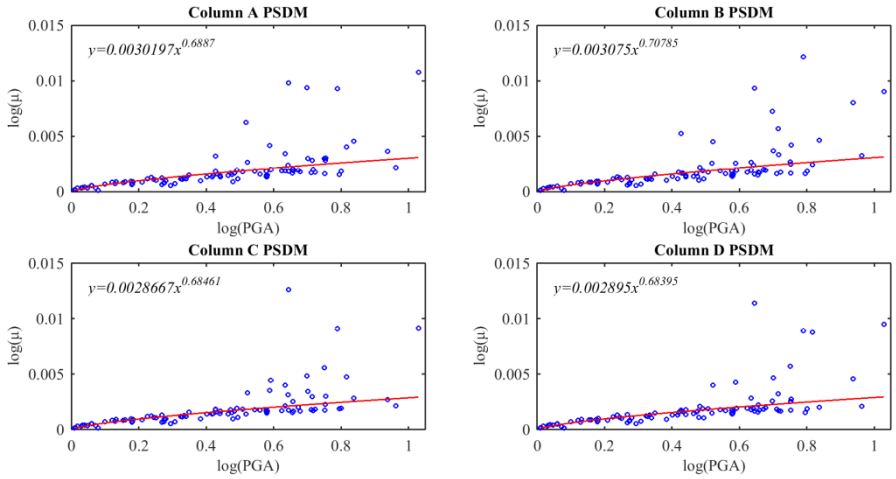

Fig. 6 Column longitudinal curvatures PSDM for the straight bridge

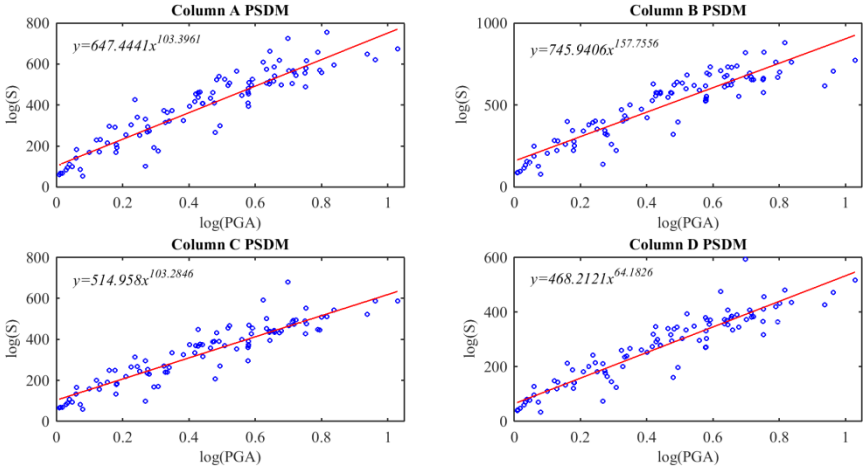

Fig. 7 PSDM of column longitudinal shear strength for the curved and skewed bridge

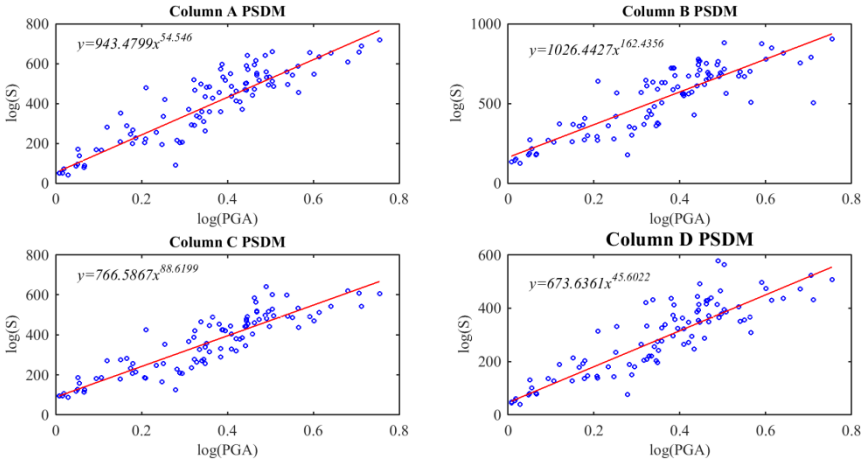

Fig. 8 PSDM of column transverse shear strength for the curved and skewed bridge

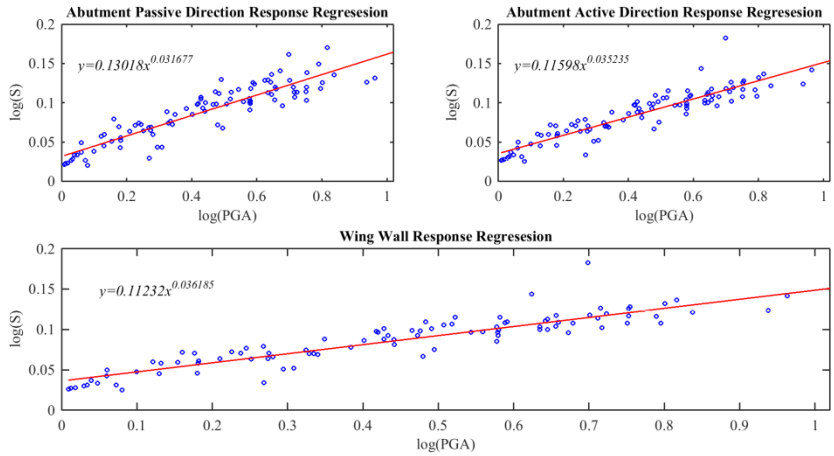

Fig. 9 PSDM of abutment deformation for the curved and skewed bridge

Table 7 Probabilistic seismic demand parameter regression of straight bridge model

Demand Response	a	b	β_d	R^2
Col-Long (A)	0.0037	0.7011	0.928425	0.6977
Col-Long (B)	0.0045	0.882	1.081222	0.8815
Col-Long (C)	0.0024	0.6472	0.802926	0.642
Col-Long (D)	0.0022	0.6368	0.765687	0.6321
Col-Trans(A)	0.0009	0.8242	0.992762	0.7984
Col-Trans(B)	0.0018	0.972	1.239829	0.9671
Col-Trans(C)	0.0006	0.7088	0.883541	0.7028
Col-Trans(D)	0.0004	0.6132	0.73181	0.6249
Shr-Long (A)	658.16	0.5896	0.63103	0.5896
Shr-Long (B)	788.93	0.5475	0.586098	0.5475
Shr-Long (C)	533.3	0.5382	0.578591	0.5382
Shr-Long (D)	452.72	0.5913	0.631935	0.5913
Shr-Trans (A)	802.69	0.6645	0.67295	0.6645
Shr-Trans (B)	880.89	0.4825	0.506952	0.4825
Shr-Trans (C)	606.61	0.4897	0.516396	0.4897
Shr-Trans (D)	552.45	0.6126	0.629689	0.6126
Abut-p (ft.)	0.152	0.4892	0.513862	0.4747
Abut-a (ft.)	0.1263	0.4419	0.444565	0.4119
Wing (ft.)	0.1263	0.4419	0.444586	0.4119

Note: Col-Long=column longitudinal curvature; Col-Trans=column transverse curvature; Shr-Long=Pier-Column Longitudinal shear strength; Shr-Trans=Pier-Column Transverse shear strength; Abut-a=abutment active deformation; Abut-p=abutment passive deformation; Wing=wing wall deformation

6.4 Fragility curve

With the previously defined limit states, fragility curves can be developed following Eq. (3).

Figs. 10(a)-10(d) list the component fragility curves for the skewed and curved bridge model, including column flexural curvatures (column A), abutment passive deformation, abutment active deformation and wing wall deformation for different limit states. For the "complete damage" limit state, fragility curves of shear forces in the longitudinal and transverse directions (column A) are also displayed.

The results shown in Fig. 10 suggest that different bridge components may dominate the fragility performance in terms of exhibiting the highest fragility under different damage states. For instance, abutment active deformation (Abut-a in Fig. 10) tend to have the highest fragility among all limit states under the light damage state. For extensive or complete damage states, the abutment however has very small probability to experience excessive deformation. For moderate and

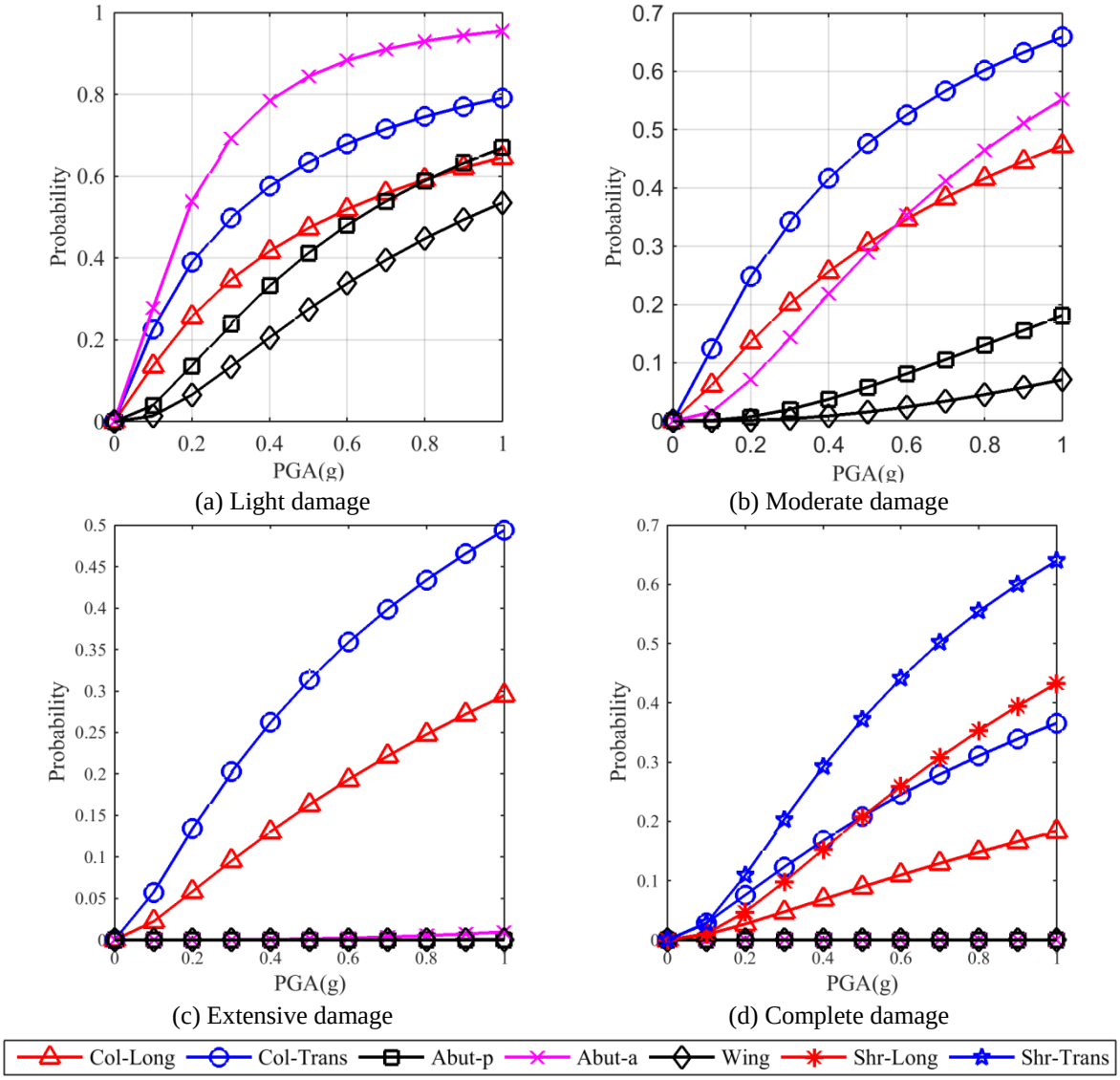

Fig. 10 Component fragility curves of the curved and skewed bridge

extensive damage states, the column transverse moment curvature has the highest fragility. When complete damage is concerned, the structural damage is governed by the column transverse shear (Shr-Trans in Fig. 10). The results also show higher fragility associated with limit states related to transverse responses of the columns for almost all damage states, highlighting the importance of bridge transverse resistance to its fragility under seismic.

7. Comparative study of critical factors

To carry out the comparative study, fragility analyses are also conducted for the straight, curved-only and skewed-only bridge models. In this section, light damage is selected as the representative damage state for the following column fragilities comparison due to its significance to low-to-moderate seismic region. Longitudinal curvatures for four individual columns (A-D) under different geometric configurations are presented in Fig. 11.

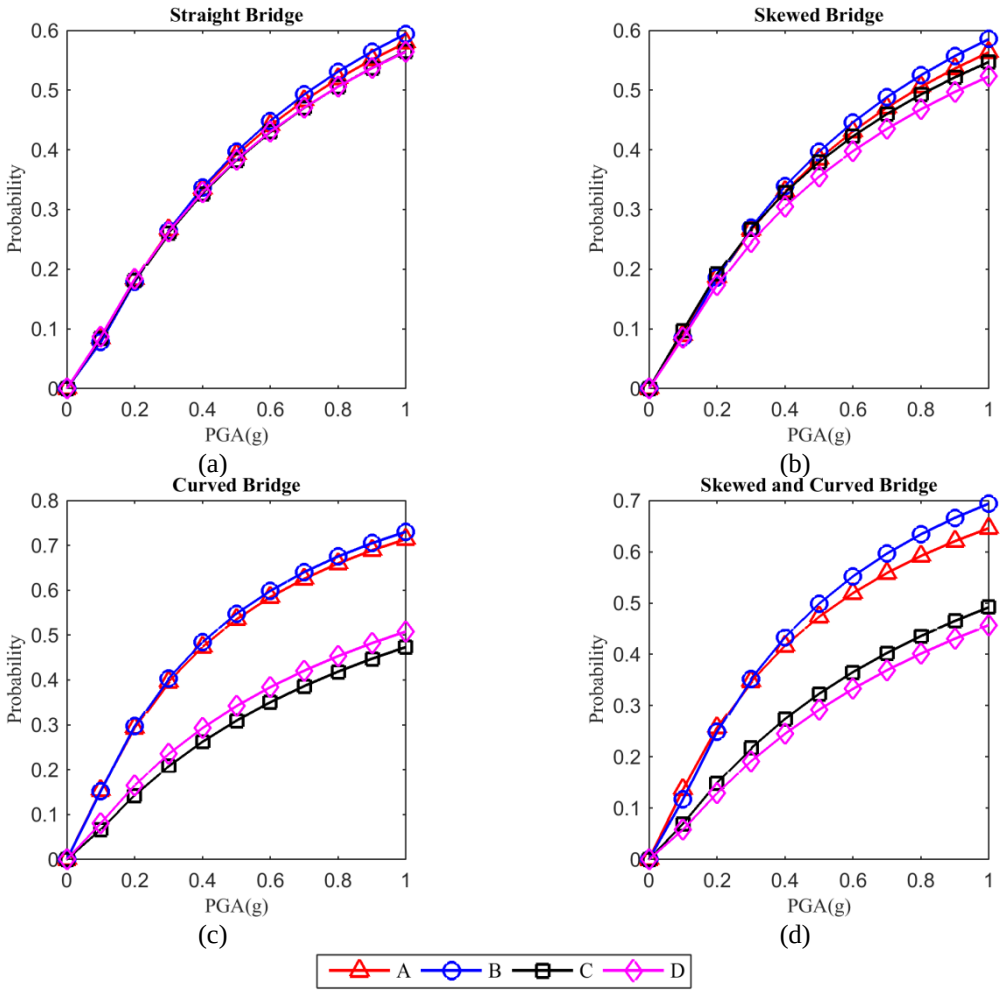

Fig. 11 Column fragility curves of longitudinal moment curvature under light damage

It is found from the results in Fig. 11 that when compared to the pretty consistent seismic performance among the columns of the straight bridge, skew and curvature cause different fragility levels among different columns. Fragility curves of the four columns of the skewed bridge are very similar by being slightly more "scattering" than those of the straight bridge at the higher range of PGA. This result is consistent with some findings made by Zakeri *et al*. (2014) in their fragility study for skewed bridges with integral abutments, where fragility curves showed negligible effect from different geometric configurations on the longitudinal moment curvatures. For the bridges with curvature (i.e., curved bridge and skewed and curved bridge models) (Figs. 11(c)-11(d)), fragilities of the interior columns of two intermediate piers (column A and B in Fig. 2) are similar, which are considerably higher than the fragility of two exterior columns (column C and D). This is because for curved bridges, its stiffness center locates at a location other than the mass center, which induces compression-bending-torsion combined load to columns when they are subject to horizontal ground motion. Such fragility difference suggests the need of picking the right column to control the design or conducting designs for each individual column for bridges with curvature.

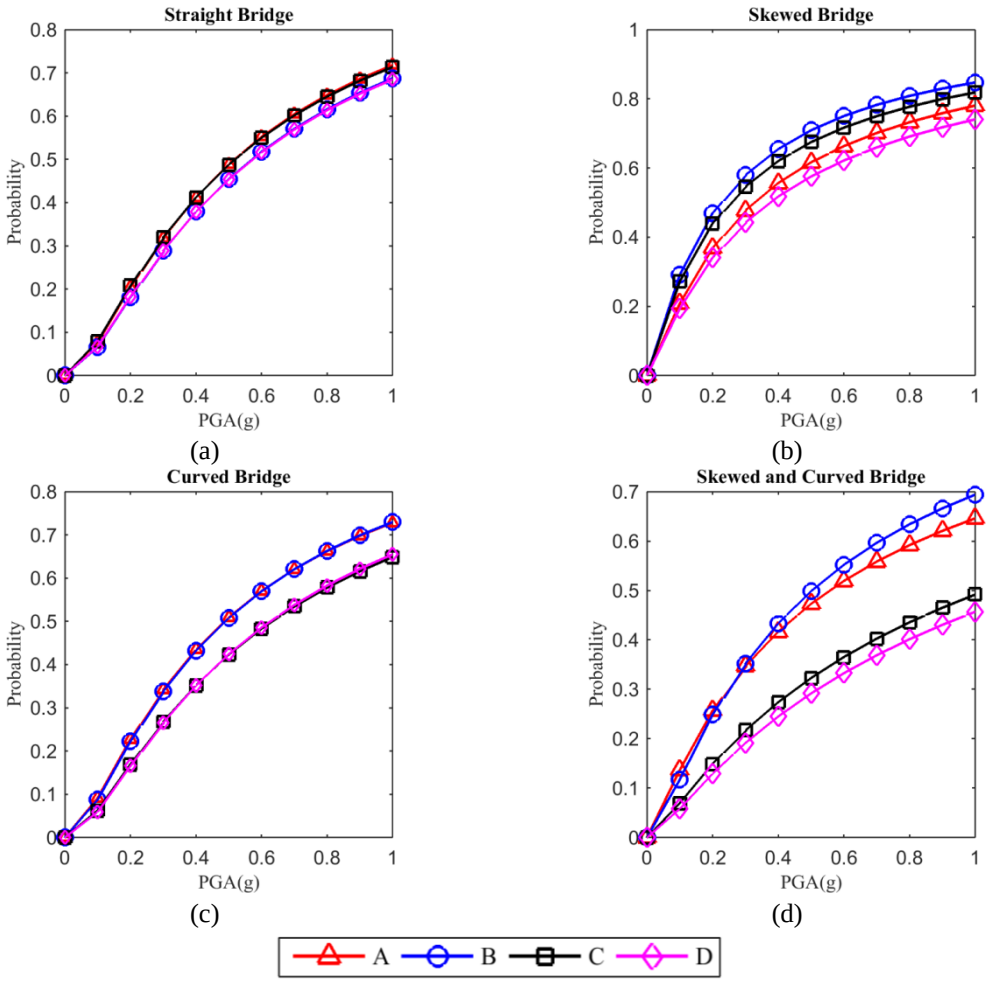

Fig. 12 Column fragility curves of transverse moment curvature under light damage

Compared to the curved bridge, the skewed and curved bridge has lower fragility in lower PGA but higher fragility in higher PGA than those of the curved bridge, respectively. Among all the bridges with different geometric configurations, the bridges with curvature (curved-only and skewed and curved bridges) have relatively higher overall fragility of the longitudinal moment curvature. Similar trend can be observed on transverse moment curvature (Fig. 12) that curved geometry causes difference on the fragility results of interior and exterior columns. In addition, the skewed nature of the bridge causes difference of fragility results between the two interior columns and also two exterior columns. For curved-only bridge (Fig. 12(c)), the two interior and two exterior columns have almost identical fragility results, respectively. Comparatively, the skewed-only bridge has the highest fragility of transverse moment curvature among all geometric configurations.

Since column B is found to have relatively higher fragility of longitudinal moment curvature than the rest columns, it is selected for demonstration in the following comparative study. Fig. 13 lists the fragility results of column B for four bridges with different geometric configurations. For each bridge, the fragility curves of four damage states are plotted. The results suggest that the fragility results of the straight bridge and skewed bridge are very similar. Bridges with curvature exhibit higher fragility than straight and skewed counterparts.

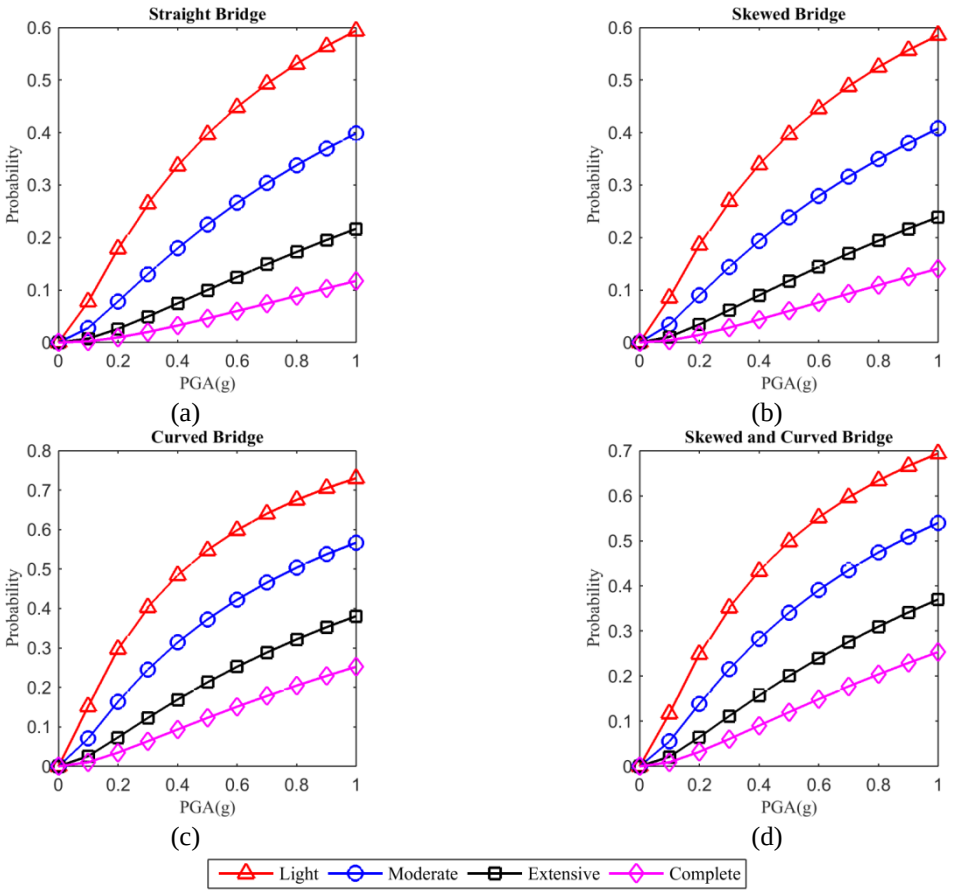

Fig. 13 Column fragility curves of longitudinal moment curvature of Column B

Fig. 14 shows the median PGA of each curve with 50% fragility of different limit states under light damage state in the longitudinal direction, and the median PGA values are inversely proportional to the component fragility. The limit state of "Abut-a" (abutment active deformation) has overall much lower median PGA than other limit states for all bridge models. The bridges with curvature are found to have lower median PGA than other bridges for column longitudinal moment curvature. For column transverse moment curvature, the bridges with skew have relatively lower median PGA. In Fig. 15, the median PGA results for moderate damage state are given for three limit states and some similar trends as the light damage level are observed. For moderate damage state, lowest median PGA is found for the limit state related to column transverse moment curvature.

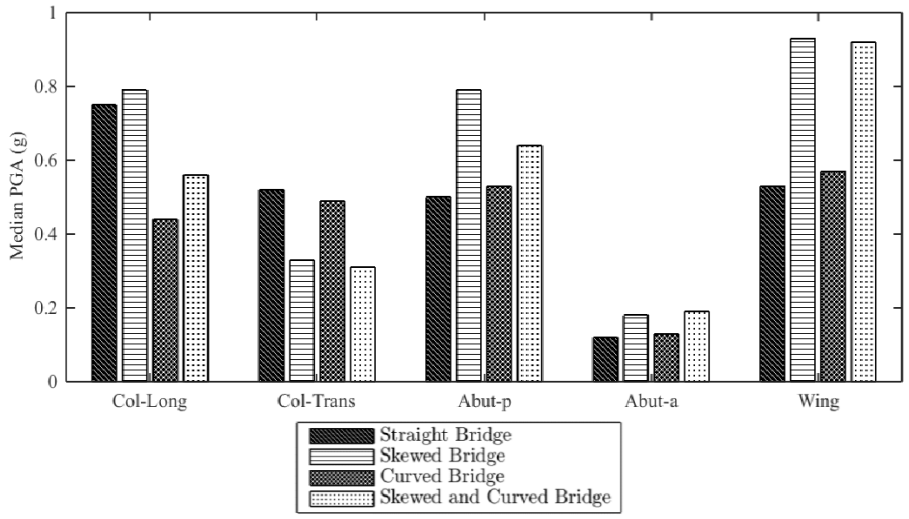

Fig. 14 Median PGA of different limit states for light damage level

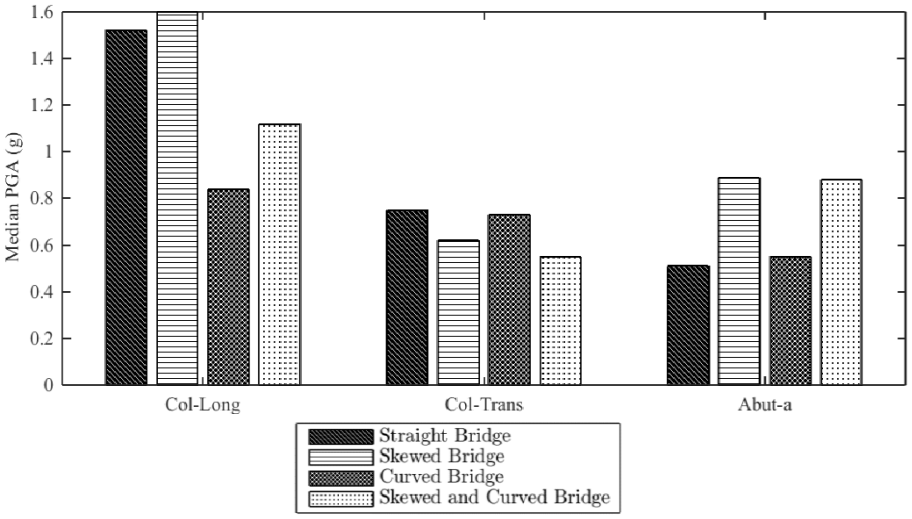

Fig. 15 Median PGA of different limit states for moderate damage level

8. Conclusions

This study investigates the seismic risk of a skewed and curved bridge in low-to-moderate seismic regions by developing analytical fragility curves. A typical 3-span concrete straight bridge located in Denver, CO was selected as the prototype bridge, from which three bridge models with complex geometric variations were modified. Based on the nonlinear FEM analysis results of these bridge models, fragility analyses were carried out considering the uncertainties of the bridge model and also ground motions. Comparative studies were also made to investigate the influences from the geometric configurations. Some main conclusions are summarized as following:

• For the skewed and curved bridge model investigated in this study, it was found that different bridge components may dominate the fragility performance in terms of exhibiting the highest fragility under different damage states. Given the complex seismic risk performance associated with curved and/or skewed configurations, a comprehensive risk assessment of bridges with complex geometric configurations is found important even in low-to-moderate seismic regions;

• For the skewed and curved bridge, columns are found to have high fragility associated with transverse demands for almost all the limit states, highlighting the importance of the transverse seismic resistance to the serviceability and safety of skewed and curved bridges. Comparatively, the bridges with curvature have overall the highest fragility of the longitudinal moment curvature, while the skewed-only bridge has the highest fragility of the transverse moment curvature;

• As compared to pretty consistent seismic performance among the columns of the straight bridge, skew and curvature nature was found to cause different fragilities on individual columns. Fragility curves for different columns of the skewed bridge are pretty similar and tend to only "scatter" in the high seismic intensity region. For the bridges with curvature, fragilities of the interior columns of two intermediate piers are similar, which are considerably higher than the fragility of two exterior columns. The skew nature causes some difference on the fragilities between two interior columns and two exterior columns, respectively. Such fragility difference among columns suggests the need of picking the right column to control the design or conducting column-specific design for individual columns of bridges with curvature;

• For light damage state, the limit state for "Abut-a" has overall much lower median PGA than other limit states for all bridge models. Bridges with curvature are found to have lower median PGA than other bridges for column longitudinal moment curvature. Bridges with skew have lower median PGA for column transverse moment curvature. For moderate damage state, lowest median PGA is found for the limit state related to column transverse moment curvature.

Acknowledgements

This study was partially sponsored by the United States Department of Transportation (through the Mountain Plains Consortium). Colorado Department of Transportation provided important information and details of the prototype bridge and the skewed and curved bridge configurations, which are greatly appreciated. It is also acknowledged that Mr. Thomas Wilson, a former graduate student, offered some help during the initial model development process. The content of this paper reflects the views of the authors, who are responsible for the facts and the accuracy of the information presented.

Reference

AASHTO (2013), LRFD Bridge Design Specifications, Customary U.S. Units, 6th Edition, with 2013 Interim Revisions

Billah, A.M., Alam, M.S. and Bhuiyan, M.R. (2012), "Fragility analysis of retrofitted multicolumn bridge bent subjected to near-fault and far-field ground motion", *J. Bridge Eng.*, **18**(10), 992-1004.

Baker, J.W. and Cornell, C.A. (2005), "A vector-valued ground motion intensity measure consisting of spectral acceleration and epsilon", *Earthq. Eng. Struct. Dyn.*, **34**(10), 1193-1217.

Baker, J.W. and Cornell, C.A. (2006), "Vector-valued ground motion intensity measures for probabilistic seismic demand analysis", Pacific Earthquake Engineering Research Center, College of Engineering, University of California, Berkeley.

Berkeley, C.S.I. (2011), Computer program SAP2000 v14. 2.4. Computers and Structures Inc., Berkeley, California.

Bavirisetty, R., Vinayagamoorthy, M. and Duan, L. (2000), "Dynamic analysis", Eds., W.-F. Chen and L. Duan, Bridge Engineering Handbook, CRC Press.

Choi, E. (2002), "Seismic analysis and retrofit of Mid-America bridges", Ph.D. thesis, Georgia Institute of Technology, Atlanta.

California Department of Transportation (2006), Caltrans Seismic Design Criteria, (1.6), 161.

Ellingwood, B. and Hwang, H. (1985), "Probabilistic descriptions of resistance of safety related structures in nuclear plants", *Nuclear Eng. Des.*, **88**(2), 169-178.

Ellingwood, B.R. and Kinali, K. (2009), "Quantifying and communicating uncertainty in seismic risk assessment", *Struct. Safe.*, **31**(2), 179-187.

Fang, J., Li, Q., Jeary, A. and Liu, D. (1999), "Damping of tall buildings: Its evaluation and probabilistic characteristics", *Struct. Des. Tall Build.*, **8**(2), 145-153.

FHWA (1995), Seismic Retrofitting Manual for Highway Bridges, Vol. FHWA-RD-94- 052. Office of Engineering and Highway Operations R&D, Federal Highway Administration, McLean, VA.

FEMA (1997), HAZUS. Earthquake loss estimation methodology. Technical Manual, National Institute of Building for the Federal Emergency Management Agency, Washington DC.

FEMA (2003), HAZUS-MH MR1: Technical Manual, Vol. Earthquake Model. Federal Emergency Management Agency, Washington DC.

Hwang, H., Jernigan, J.B. and Lin, Y.W. (2000), "Evaluation of seismic damage to Memphis bridges and highway systems", *J. Bridge Eng.*, **5**(4), 322-330.

Kowalsky, M.J. and Priestley, M.N. (2000), "Improved analytical model for shear strength of circular reinforced concrete columns in seismic regions", *ACI Struct. J.*, **97**(3), 388-396.

Kwon, O.S. and Elnashai, A.S. (2007), "Fragility analysis of a bridge with consideration of Soil-Structure-Interaction using multi-platform analysis", *Structural Engineering Research Frontiers*, ASCE.

MacGregor, J.G., Wight, J.K., Teng, S. and Irawan, P. (1997), "Reinforced concrete: mechanics and design (Vol. 3)", Upper Saddle River, NJ: Prentice Hall.

Mackie, K.R. and Stojadinović, B. (2007), "Performance-based seismic bridge design for damage and loss limit states", *Earthq. Eng. Struct. Dyn.*, **36**(13), 1953-1971.

Matthews, V. (2003), "The challenges of evaluating earthquake hazard in Colorado", Engineering Geology in Colorado: Contributions, Trends, and Case Histories.

Maragakis, E. (1984), "A model for the rigid body motions of skew bridge".

Mwafy, A.M. and Elnashai, A.S. (2007), "Assessment of seismic integrity of multi-span curved bridges in mid-America".

Neves, L.A., Frangopol, D.M. and Cruz, P.J. (2006), "Probabilistic lifetime-oriented multi-objective optimization of bridge maintenance: Single maintenance type", *J. Struct. Eng.*, **132**(6), 991-1005.

Nielson, B.G. (2005), "Analytical fragility curves for highway bridges in moderate seismic zones", Ph.D. dissertation, Georgia Institute of Technology.

Nielson, B.G. and DesRoches, R. (2007), "Seismic fragility methodology for highway bridges using a

component level approach", *Earthq. Eng. Struct. Dyn.*, **36**(6), 823-839.
Pan, Y., Agrawal, A.K. and Ghosn, M. (2007), "Seismic fragility of continuous steel highway bridges in New York State", *J. Bridge Eng.*, **12**(6), 689-699.
Padgett, J.E. and DesRoches, R. (2007), "Sensitivity of seismic response and fragility to parameter uncertainty", *J. Struct. Eng.*, **133**(12), 1710-1718.
Padgett, J.E. and DesRoches, R. (2008), "Methodology for the development of analytical fragility curves for retrofitted bridges", *Earthq. Eng. Struct. Dyn.*, **37**(8), 1157-1174.
Priestley, M.J.N., Seible, F. and Calvi, G.M. (1996), *Seismic Design and Retrofit of Bridges*, John Wiley &Sons, New York, USA
Rix, G.J. and Fernandez-Leon, J.A. (2004), "Synthetic ground motions for Memphis", TN. http://www. ce. gatech. edu/research/mae_ground_ motionæ (Jul. 5, 2008).
Sullivan, I. and Nielson, B.G. (2010), "Sensitivity analysis of seismic fragility curves for skewed multi-span simply supported steel girder bridges", *Proceedings of 19th Analysis and Computation Specialty Conference*, Structures Congress.
Saiidi, M. and Orie, D. (1992), "Earthquake design forces in regular highway bridges", *Comput. Struct.*, **44**(5), 1047-1054.
Shinozuka, M., Kim, S.H., Kushiyama, S. and Yi, J.H. (2002), "Fragility curves of concrete bridges retrofitted by column jacketing", *Earthq. Eng. Eng. Vib.*, **1**(2), 195-205.
Sucuoğlu, H. and Erberik, A. (2004), "Energy-based hysteresis and damage models for deteriorating systems", *Earthq. Eng. Struct. Dyn.*, **33**(1), 69-88.
Vickery, P.J., Skerlj, P.F., Lin, J., Twisdale Jr, L.A., Young, M.A. and Lavelle, F.M. (2006), "HAZUS-MH hurricane model methodology. II: Damage and loss estimation", *Natl. Haz. Rev.*, **7**(2), 94-103.
WSDOT (2002), Design Manual, Program Development Division, Washington State Department of Transportation, Olympia, WA. http://www.wsdot.wa.gov/Publications/Manuals/M22-01.htm
Wen, Y.K. and Wu, C.L. (2001), "Uniform hazard ground motions for Mid-America cities", *Earthq. Spectra*, **17**(2), 359-384.
Wilson, T., Mahmoud, H. and Chen, S. (2014), "Seismic performance of skewed and curved reinforced concrete bridges in mountainous states", *Eng. Struct.*, **70**, 158-167.
Wilson, T., Chen, S. and Mahmoud, H. (2015), "Analytical case study on the seismic performance of a curved and skewed reinforced concrete bridge under vertical ground motion", *Eng. Struct.*, **100**, 128-136.
Xiao, Y. and Ma, R. (1997), "Seismic retrofit of RC circular columns using prefabricated composite jacketing", *J. Struct. Eng.*, **123**(10), 1357-1364.
Zhang, J. and Huo, Y. (2009), "Evaluating effectiveness and optimum design of isolation devices for highway bridges using the fragility function method", *Eng. Struct.*, **31**(8), 1648-1660.
Zakeri, B., Padgett, J.E. and Amiri, G.G. (2014), "Fragility analysis of skewed single frame concrete box girder bridges", *J. Perform. Constr. Facil.*, **28**(3), 571-582.

CC